Journal of Structural Geology, Vol. 11, No. 1/2, pp. 1 to 14, 1989
Printed in Great Britain

0191-8141/89 $03.00 + 0.00

Earthquake faulting as a structural process

RICHARD H. SIBSON

Department of Geological Sciences, University of California, Santa Barbara, CA 93106, U.S.A.

(*Received* 11 *April* 1988; *accepted* 13 *October* 1988)

Abstract—Structural geology is concerned with the history of movement in the Earth's crust and the processes by which displacements occur. In the upper one third to one half of deforming continental crust, displacement is accommodated largely by seismic slip increments on existing faults. It follows that earthquakes and related processes are an integral part of structural geology. Traditionally, structural geologists have been preoccupied with the complexity of the finite deformation within fault zones and with the stress states prevailing at the initiation of faults in intact crust. Future structural work should be directed more towards understanding the dynamic character of fault reactivation during incremental slip, and related effects. Questions of interest include rheological and geometrical controls on the initiation, perturbation and termination of ruptures; directivity effects associated with rupture propagation; the recognition of structures resulting from repeated stress cycling within seismogenic crust; and identification of structural features diagnostic of shear stress levels during faulting. Structures arising from the inter-relationships between slip episodes and induced fluid flow are of special importance, because these dynamic fault processes appear influential in the development of much fault-hosted mineralization.

Mesothermal gold–quartz lodes hosted in high-angle reverse shear zones of mixed brittle–ductile character form illustrative examples of structures that, arguably, can only be interpreted by seismo-structural analysis embodying the concepts listed above.

INTRODUCTION

IT IS now clear that much of the displacement occurring in the upper half of actively deforming continental crust is accomplished by earthquake faulting, and that only the larger earthquakes within such regions contribute significantly to the displacement (e.g. Hyndman & Weichert 1983). Much of the high-level folding in the crust may also be a consequence of fault displacements and, in at least some instances, the incremental amplification of such folds accompanies seismic slip episodes on the faults (King & Vita-Finzi 1981, Stein & King 1984). Geologists and seismologists clearly have much to contribute to each other's understanding of fault processes, but major communication problems have arisen in the past through inherently different perceptions of the fundamental character of faults.

Traditionally, seismologists have been preoccupied with the effects of incremental slip within fault systems; structural geologists with the total displacement across faults and the finite deformation state associated with them, which may be very complex. In their initial training, geologists are generally taught to analyse finite fault displacements in terms of rigid block motions, with constant slip vectors across perfectly planar shear dislocations. None of these assumptions is warranted, neither for an isolated slip increment during an earthquake, nor for long-term displacements. A related question is the extent to which faulting is truly a 'brittle' process. The problem is nicely illustrated by considering the incremental and finite aspect ratios for faults. For earthquake ruptures, the ratio between maximum seismic slip, u_s, and the rupture length, L_s, generally lies in the range:

$$10^{-4} > u_s/L_s > 10^{-5} \qquad (1)$$

(Rikitake 1975). This ratio approximates the change in shear strain accompanying propagation of the rupture. The value is so small, well within the elastic limit of rocks, that it is natural for seismologists to think of faults as brittle shear fractures within a perfectly elastic surrounding medium. To field geologists, however, faults appear as much more ductile structures because finite displacements on faults die out more quickly. The ratio of maximum finite displacement, u_f, to total fault length, L_f, tends to increase as a fault matures (Walsh & Watterson 1988) and may eventually reach values,

$$u_f/L_f \sim 0.1. \qquad (2)$$

This implies that permanent strains of the same order invariably develop around the terminations of faults (King 1978, Moore & du Bray 1978, Watterson 1986). Mutual misunderstanding is exacerbated because, while to a seismologist a 10% strain is extremely large, to a structural geologist it is barely measurable!

Another traditional concern of structural geologists has been the stress state prevailing at the time of fault initiation. Along with this goes a tendency to interpret minor structures associated with faults in terms of static stress fields. Yet it is now over three quarters of a century since Reid's (1911) recognition of the elastic rebound of strained crust as the fundamental earthquake mechanism, with its implications of continual stress cycling in the vicinity of active crustal faults. Plate tectonics works, moreover, because significant displacements are concentrated on well-localized fault zones at plate boundaries, which persist for lengthy time periods through continual reactivation. However, while stress cycling accompanying episodic reactivation is likely to be the norm in the vicinity of faults, there has been little recognition of related structural features.

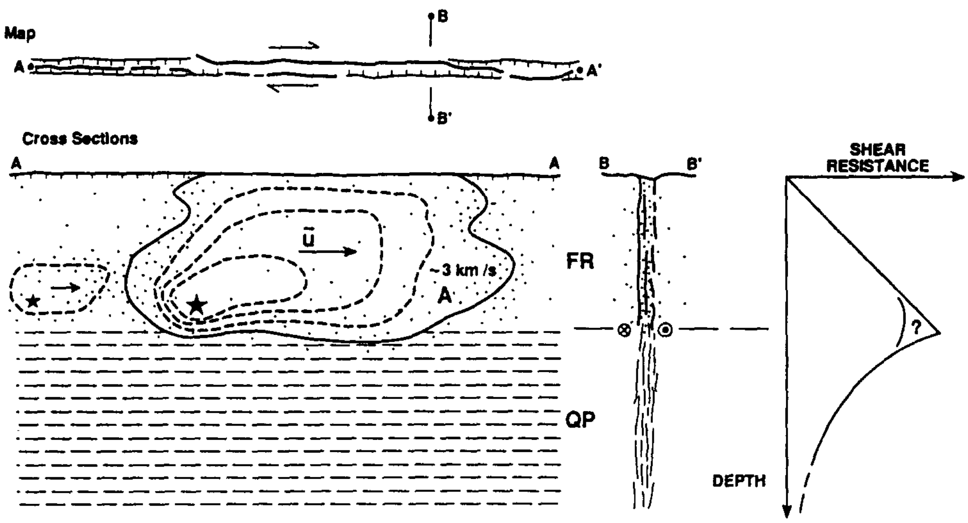

Fig. 1. Strike-slip earthquake rupturing within the seismogenic regime defined by background microseismicity and aftershock activity, shown in relation to a composite profile of fault shear resistance versus depth which peaks in the vicinity of the transition from unstable frictional (FR) faulting to localized quasi-plastic (QP) shearing flow (after Sibson 1986b). Longitudinal fault section shows large ruptures expanding over the fault surface at ~3 km s^{-1} from nucleation sites (stars) in the vicinity of the FR/QP transition. Mean slip, $\bar{u}$, is averaged over a final rupture area, A, which occupies all or part of the seismogenic zone.

Modern seismological studies of shallow crustal earthquakes thus pose many interesting questions for future research into the structural geology of fault zones. This paper seeks to indicate some of the directions which such research might take.

THE SEISMOGENIC REGIME

Increasing deployment of high-density seismograph networks, coupled with the more sophisticated techniques now available for teleseismic determination of focal depths, make it clear that seismic activity is largely restricted to the upper one third to one half of deforming continental crust, its lower bound apparently governed by the onset of greenschist facies metamorphic conditions at temperatures of ~300–350°C (Chen & Molnar 1983, Sibson 1983). This gives rise to the concept of a *seismogenic regime* defined by background microearthquake activity as illustrated in Fig. 1. From a mechanical viewpoint, the base of the seismogenic regime is thought to represent a transition zone from unstable frictional (FR) faulting to quasi-plastic (QP) shearing flow localized in mylonite belts. It holds special mechanical significance as the region of inferred peak shear resistance where larger earthquake ruptures (M>6*) tend to nucleate. Mostly, these larger earthquakes rupture upwards and laterally so that their aftershocks also are largely restricted to the upper crust. There is, however, some evidence that these bigger events also rupture some distance downwards beneath the background seismogenic zone (Strehlau 1986, Scholz 1988). Deformation around the base of the seismogenic zone in the vicinity of the FR/QP transition is thus likely to involve a complex mixture of continuous and discontinuous shearing.

*Note that throughout this paper, the earthquake magnitude scale referred to is moment-derived magnitude, M, based on the moment-magnitude relationship of Hanks & Kanamori (1979). This corresponds to local magnitude over the range $3 < M_L < 7$ and surface wave magnitude over the range $5 < M_s < 7.5$.

Size-frequency distribution of earthquake ruptures

In any seismically active region, the relative frequency of different sized earthquakes follows the cumulative Gutenberg–Richter (1944) relationship,

$$\log_{10} N(\mathrm{M}) = a - b\mathrm{M} , \quad (3)$$

where N(M) is the number of earthquakes of magnitude greater or equal to M, and a and b are constants characteristic of the region. In most regions the b-value is about unity, so that earthquakes generally become about 10 times more frequent for every unit decrease in magnitude. In a region of moderate seismic activity such as New Zealand, for example, an M8 earthquake tends to occur about every 100 years on average, an M7 shock occurs roughly every 10 years, and within 1 year, one can expect on average perhaps one M6 earthquake, ~10 M5 events, ~100 M4 events and so on. This empirical statistical relationship cannot, of course, be extended indefinitely upwards; in any particular region there appears to be a maximum magnitude above which the distribution is truncated (Molnar 1979).

Over an enormous scale range, the drops in shear stress ($\Delta\tau$) associated with crustal earthquakes are remarkably uniform. In general, $\Delta\tau$ is the range 1–100 bars with a logarithmic mean at ~30 bars (Kanamori & Anderson 1975, Hanks 1977), corresponding to the strain changes observed in the vicinity of ruptures (equation 1). Given this near constancy of stress drop, one can obtain some grasp of typical rupture parameters associated with earthquakes of different magnitude (Table 1). Note further, that under constant stress drop

Table 1. Structural characteristics and relative frequency of earthquake ruptures of different sizes. Rupture area (A), fault dimensions (length, L, and down-dip width, W) and mean slip ($\bar{u}$) have been calculated from elastic dislocation theory (Kanamori & Anderson 1975) for circular ruptures of radius $L/2$ with $\Delta\tau$ = 30 bars, using the moment–magnitude relationship of Hanks & Kanamori (1979). Bracketed values are approximate fault dimensions assuming the larger ruptures to be confined to a vertical fault in a 15 km deep seismogenic zone

Magnitude M	Average slip $\bar{u}$	Rupture length or width L or W	Rupture area $A \approx LW$	Relative frequency
M8	~4 m	~100 km (650 km/15 km)	$\sim 10^4$ km^2	N yr^{-1}
M7	~1 m	~30 km (60 km/15 km)	$\sim 10^3$ km^2	$\sim 10N$ yr^{-1}
M6	~40 cm	~10 km	$\sim 10^2$ km^2	$\sim 10^2N$ yr^{-1}
M5	~10 cm	~3 km	~10 km^2	$\sim 10^3N$ yr^{-1}
M4	~4 cm	~1 km	~1 km^2	$\sim 10^4N$ yr^{-1}
M3	~1 cm	~300 m	$\sim 10^5$ m^2	$\sim 10^5N$ yr^{-1}
M2	~4 mm	~100 m	$\sim 10^4$ m^2	$\sim 10^6N$ yr^{-1}
M1	~1 mm	~30 m	$\sim 10^3$ m^2	$\sim 10^7N$ yr^{-1}

conditions, the earthquake frequency–magnitude relationship for a region can also be interpreted as a size–frequency distribution of rupture areas of form:

$$N(\mathrm{M}) \propto 1/A \tag{4}$$

(Hanks 1977, Andrews 1980).

'Characteristic earthquake' concept

A principal revelation of the paleoseismic studies of active fault zones that have burgeoned over the past 10 years or so has been the recognition that the standard frequency–magnitude relationship does not hold for individual fault zones (Wesnousky *et al.* 1983, Schwartz & Coppersmith 1984). Rather, there is accumulating evidence that particular faults, or segments of major fault zones, often rupture at fairly regular intervals in maximum magnitude events characteristic of that particular fault segment. One notable example is the ~25 km long Parkfield–Cholame segment of the San Andreas Fault (Fig. 2) which is believed to have ruptured in

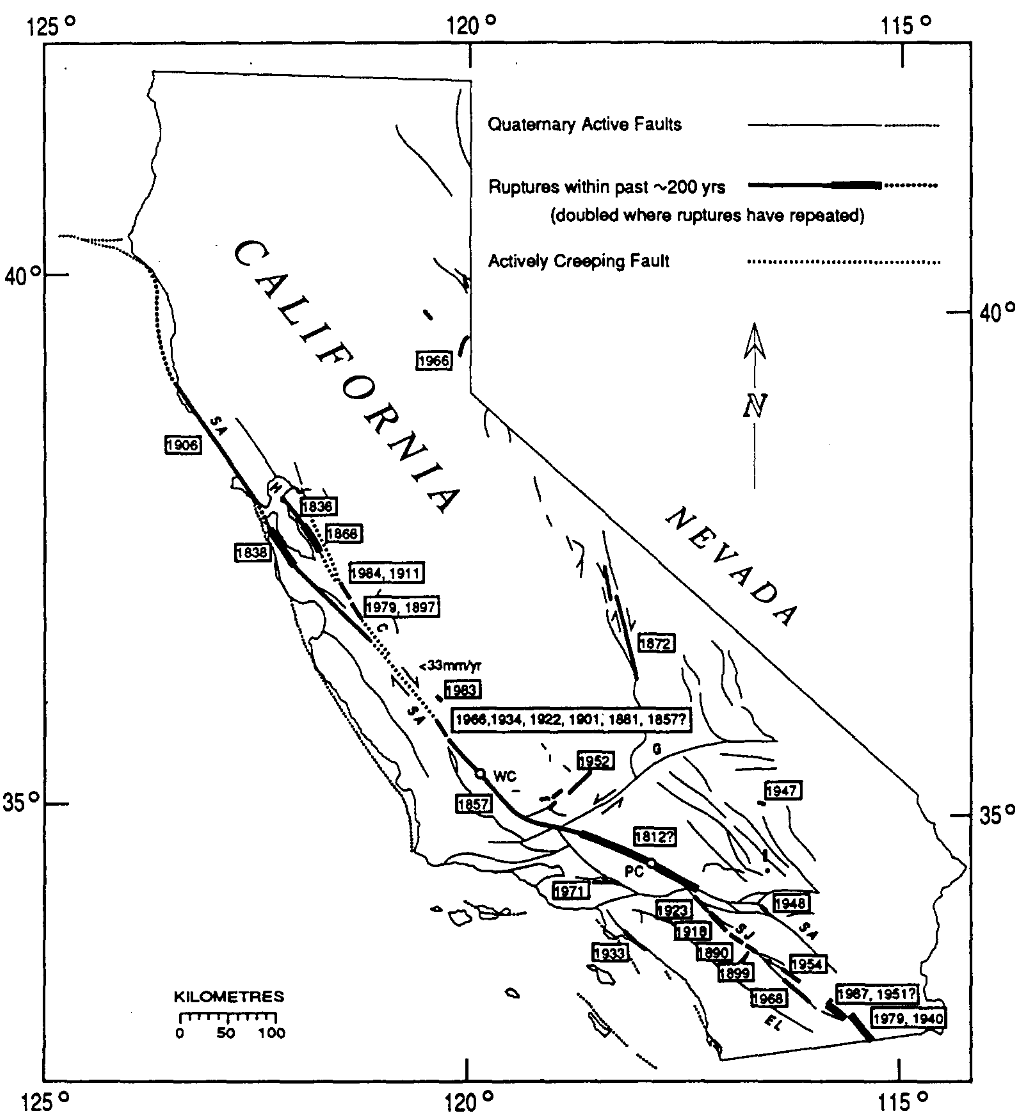

Fig. 2. Sketch map of the San Andreas fault system in California illustrating segmentation. C — Calveras Fault, EL — Elsinore Fault, G — Garlock Fault, H — Hayward Fault, SA — San Andreas Fault, SJ — San Jacinto Fault; WC and PC are, respectively, the Wallace Creek and Pallet Creek paleoseismic trench sites. Earthquakes plotted are historical events whose ruptures are reasonably well-defined from recorded surface breaks, isoseismals, or well-defined aftershock zones (updated from Jennings 1975 and Scholz 1977). Note that the map is inevitably incomplete, and that the data on rupture extent becomes very uncertain for events more than 50 years old.

similar ~M6 earthquakes in 1857 (as a foreshock to the ~M8 'big-bend' earthquake), 1881, 1901, 1922, 1934 and 1966 (Bakun & McEvilly 1984). While 'perfect' characteristic earthquake behavior by no means always occurs (particular fault segments have been known to rupture in different sized events), it is clear that the intervening number of lesser events on the same fault segment between successive large events is generally much less than that expected from the frequency–magnitude relationship. The frequency–magnitude relationship for a region thus seems to arise through the statistical tendency for a population of fault segments, each with its own characteristic rupture size, to develop in accordance with equation (4).

Characteristic earthquake behavior has highly important structural implications. It demands the existence of structural controls which govern the initiation and termination of characteristic earthquake ruptures at particular sites. These controls must persist for extended time periods through successive earthquake cycles.

Stress levels and stress cycling within the seismogenic regime

Faulting occurs to relieve accumulated shear stress on faults. As previously discussed, the drop in shear stress accompanying seismic faulting is well established from seismology and geodetic measurements. Within the seismogenic portions of a fault zone exhibiting characteristic earthquake behavior, shear stress may therefore be expected to fluctuate in crude saw-tooth oscillations of amplitude, $\Delta\tau \leqslant 100$ bars (Fig. 3). The cycle may be subdivided into four phases: an α-phase of secular, mainly elastic strain accumulation; a β-phase of possible preseismic anelastic deformation, perhaps involving foreshock activity and accelerating precursory slip; a

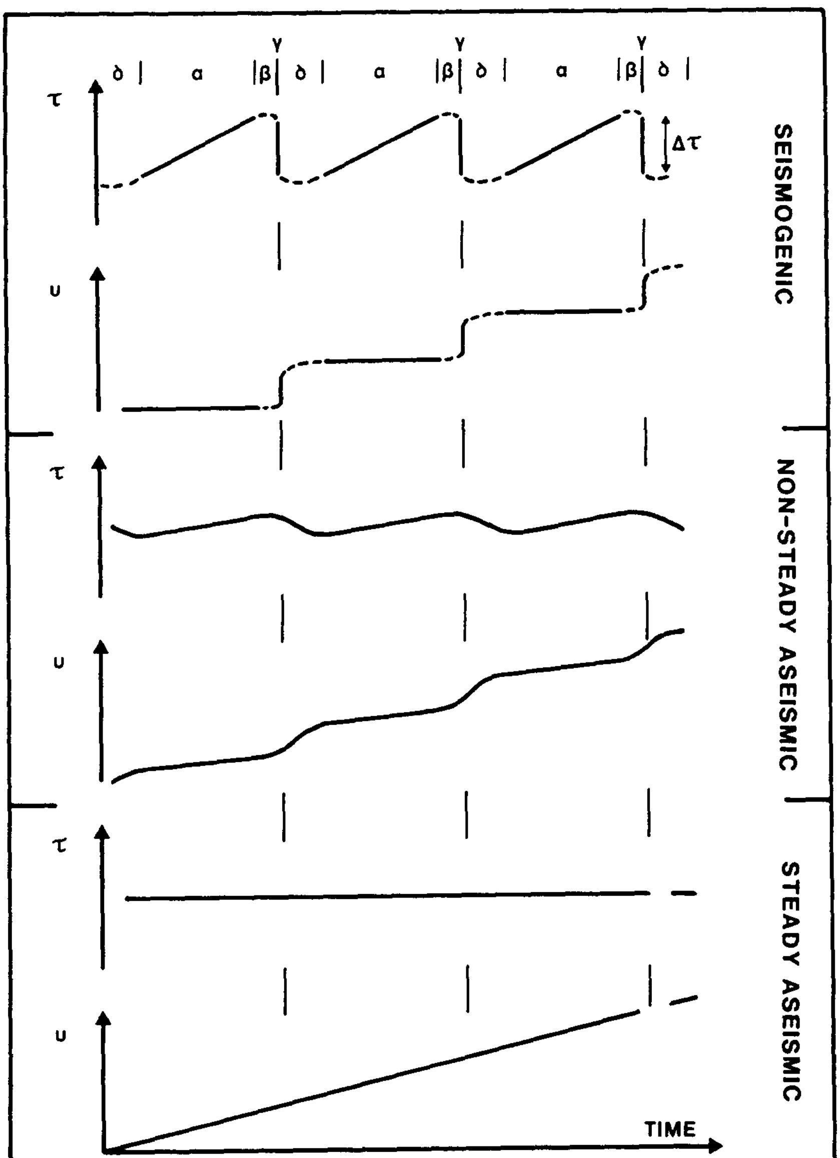

Fig. 3. Temporal variations in shear stress (τ) and displacement (u) inferred for seismically and aseismically slipping portions of crustal fault zones (after Sibson 1986a). The earthquake stress cycle is subdivided into an α-phase of secular strain accumulation, a β-phase of possible preseismic anelastic deformation, a γ coseismic phase of mainshock rupturing accompanied by a stress drop, $\Delta\tau$, and a δ-phase of afterslip and decaying aftershock activity.

coseismic γ-phase of mainshock rupturing and energy release; and a postseismic δ-phase of decelerating afterslip and aftershock activity decaying inversely with time. In contrast, steady aseismic shearing such as occurs along the creeping portions of the San Andreas Fault in central California (Burford & Harsh 1980), or is inferred at depth beneath the seismogenic regime, probably takes place under near-constant shear stress. Transitional behavior with damped stress oscillations must occur in intermediate regions.

Oscillating levels of shear stress must also extend considerable distances laterally into the crust surrounding seismically active fault zones. The extent of the region of perturbed stress depends critically on the dimensions of the mainshock rupture. For a crust transected by a very long strike-slip rupture extending through the seismogenic regime on a vertical fault, dislocation modelling shows that the coseismic strain (and stress) change drops to about 50% of the value at the fault at distances comparable to the depth of the seismogenic zone (or fault width); say 10–15 km each side of the fault trace (Mavko 1981). If we consider the situation in southern California (Fig. 2), where several major active strike-slip faults are spaced ~40 km apart, we may reasonably infer that the entire upper crust is subject to some degree of stress cycling from events on one or other of the faults. Stress-dependent processes such as fluid flow through fracture networks are likely to fluctuate in step with the stress cycling. From the viewpoint of interpreting structural and textural overprinting, one may note that the traditional practice of deciphering relationships between minor structures in terms of a regional deformation sequence (D_1, D_2, D_3, etc.) may come to grief in areas where stress cycling has been prevalent, and diverse structural features have developed or amplified at different stages of the repeating cycle.

The extent to which the regional stress field is perturbed by such stress changes must depend on the ratio of stress drop to the absolute level of shear stress driving the faults. Unfortunately, the level of shear stress initiating slip events within the seismogenic regime (τ_i) remains uncertain. Two end-member schools of thought (Hanks & Raleigh 1980) are:

(1) τ_i is ~100 bars, comparable to the larger observed stress drops, so that $\Delta\tau/\tau_i \rightarrow 1$. In this case, the seismic efficiency of rupturing is high with a large proportion of the released strain energy radiated as seismic waves.

(2) τ_i is ~1 kbar, so that $\Delta\tau/\tau_i \leqslant 0.1$ and the seismic efficiency is low, with much energy dissipated on the fault during slip events.

In the first case, stress trajectories in the vicinity of the fault are likely to be strongly perturbed after each slip event; in the latter, the effects are likely to be less severe. As a possible example of the first situation, consider the 1984 M6.2 Morgan Hill earthquake. Following an ~25 km long, pure strike-slip mainshock rupture along the NW–SE Calaveras Fault, off-fault aftershocks involved a mixture of dextral strike-slip faulting on N–S-trending subsidiary faults and thrusting on planes striking parallel to the main rupture. Both types of aftershock activity are consistent with NE–SW compression, suggesting that shear stress along the Calaveras Fault had been almost totally relieved by the main shock (Oppenheimer *et al.* 1988).

EARTHQUAKE RUPTURE PROCESSES

Although here I restrict attention to strike-slip rupturing, because of the comparative ease with which seismological information is related to structural irregularities for this faulting mode, it should be noted that most of the concepts developed are equally applicable to dip-slip faulting.

The 1979 *Imperial Valley earthquake*

As an example of the detailed information that is likely to become increasingly available from modern seismological studies, consider the 1979 M6.5 earthquake which occurred on the Imperial Fault, part of the transform system linking the southern San Andreas Fault through to the spreading centres in the Gulf of California (Fig. 2). This right-lateral strike-slip rupture is particularly instructive because: (i) the rupture was 'caught' in the middle of a dense array of seismographs and strong motion instruments; and (ii) details of rupture geometry and its relationship to aftershock distribution are most easily appreciated for horizontally propagating strike-slip ruptures. Data from the array were modelled by Archuleta (1984) to reveal details of the rupture process on the Imperial and Brawley faults (Fig. 4). While the results are to some extent non-unique and model dependent, they serve to illustrate the general complexity of a single seismic slip event. In summary the following six points are notable.

(1) The rupture nucleated at a depth of about 8 km and propagated unilaterally northwestwards on the Imperial Fault, triggering some slip on the Brawley fault splay, but continuing for a total rupture length of ~35 km. Surface faulting was only evident along the northwestern two thirds of the rupture, and along the Brawley Fault. Silver & Masuda (1985) argue, however, for some degree of bilateral rupturing with minor subsurface propagation to the southeast as well.

(2) Advance of the rupture front was highly irregular although the average rupture velocity stayed close to the shear wave velocity (~3 km s^{-1}), so that the total duration of faulting was about 12 s.

(3) Coseismic strike-slip varied greatly over the fault surface but averaged ~0.4 m. Subordinate components of normal slip occurred on the northwest of the Imperial fault rupture and on the Brawley Fault.

(4) At any point on the rupture surface the duration of slip, while highly variable, lasted no more than 2 s. Thus fault slip at any instant during rupture propagation, was restricted to a band extending only a few kilometers behind the advancing rupture front (Fig. 4b).

(5) Aftershock activity was concentrated in a rhomboidal area adjacent to the tip of the main rupture in the

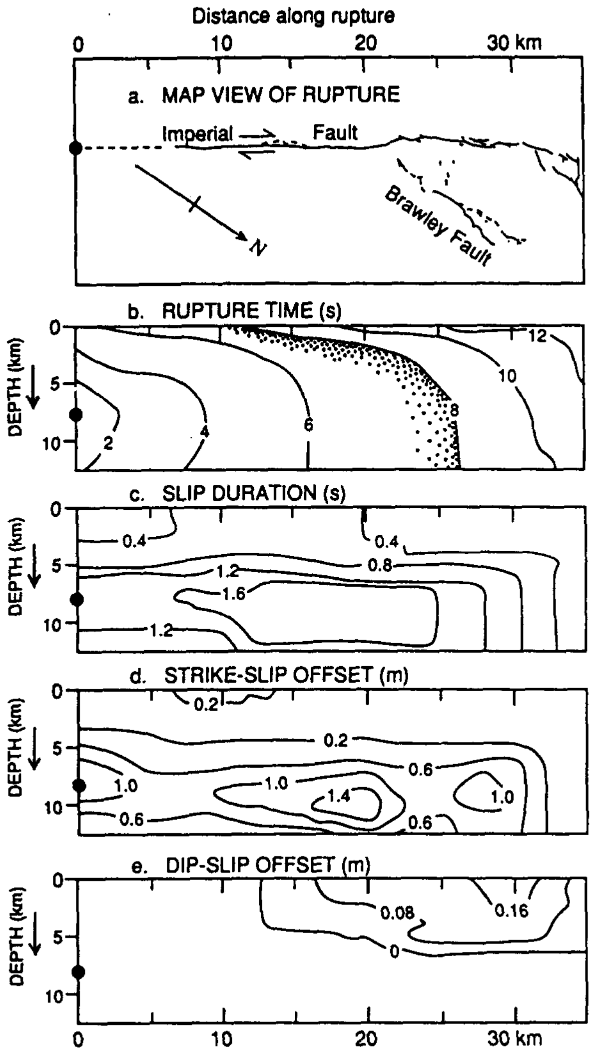

Fig. 4. 1979 Imperial Valley rupture (after Archuleta 1984): (a) Map of rupture trace; (b–e) Longitudinal sections along the rupture, showing (b) advance of rupture front with time, t (stippled area approximates slipping area behind rupture front at t = 8 s); (c) duration slip contoured over the rupture surface; (d) final strike-slip offset; and (e) final dip-slip offset. Solid circle represents rupture epicentre (a) or hypocentre (b–e).

first few hours after the earthquake (Johnson & Hutton 1982). Activity continued for weeks after the mainshock, becoming more dispersed with time. Significant afterslip occurred along the surface rupture trace over a comparable time period.

(6) The repeat time for similar events on the Imperial Fault is several tens of years (the fault last ruptured in a somewhat larger event in 1940).

Note that after some 40 years of elastic accumulation in the surrounding rocks, fault slip averaging 0.4 m was accomplished at any one point in less than 2 s, with the entire rupture process complete in an interval of only 12 s! Following the decay of afterslip and aftershock activity over a period of months, the fault will be likely to remain quiescent until the next major slip event some tens of years from now.

Rupture complexity and segmentation

Even if attention is restricted to horizontally propagating strike-slip ruptures (Fig. 5), the surface rupture traces of moderate to large earthquakes are generally irregular and complex (Vedder & Wallace 1973, Tchalenko & Berberian 1975, Segall & Pollard 1980). While heterogeneity occurs over a tremendous scale range, concepts of self-similar fault behavior (King 1983) suggest that larger earthquake ruptures, our main concern here, are significantly affected only by the larger heterogeneities with cross-strike scale of hundreds of meters to kilometers. Precision aftershock studies suggest that in at least some instances, these structural irregularities extend through the seismogenic regime to depths of ~10 km (Reasenberg & Ellsworth 1982). This is supported by studies of exhumed ancient fault zones (Sibson 1986b).

While composite structures and more complex three-dimensional linkage structures undoubtedly exist, two main classes of irregularity transverse to the direction of rupture propagation may be recognized; *fault jogs* linking en échelon fault segments, and *isolated fault bends* (Fig. 6). Within these two basic classes, structures are usefully classified as *dilational* or *antidilational* depending on the tendency for areal increase or reduction, respectively, associated with the incremental slip transfer accompanying rupture propagation across the irregularity.

Because the interaction of earthquake ruptures with fault irregularities depends only on the incremental deformation at the tip of the propagating rupture, an interesting *directivity* effect may be noted in the case of isolated fault bends (Fig. 7). For a rupture approaching the bend from the left, incremental slip transfer at the rupture tip will tend to dilate the fault segment across the bend, whereas for a rupture approaching from the right, the fault segment across the bend will experience increased compression. Evidence is accumulating that such directivity effects may have important consequences for rupture propagation and termination, and for related fluid redistribution.

Aftershock activity in relation to rupture geometry and fluid redistribution

Aftershock distributions reveal the extent of subsidiary deformation associated with earthquake rupturing. Their rate of occurrence generally decays hyperbolically with time after the mainshock (Omori's Law). For a large event (e.g. ~M7) detectable aftershocks may occur initially at rates of thousands per day but after a few months their frequency typically diminishes to perhaps 10 or so per day (Gibowicz 1973). High precision aftershock studies (epicentral and focal depth uncertainties < 1 km) following moderate to large ruptures have begun to reveal consistent relationships between the aftershock concentrations and irregularities in mainshock ruptures. These studies are most effective for strike-slip ruptures where epicentral distributions define off-fault deformation in map view. Some general observations are: (i) for buried ruptures that have not broken through to the surface, aftershocks tend to concentrate around the periphery of the mainshock rupture, and to

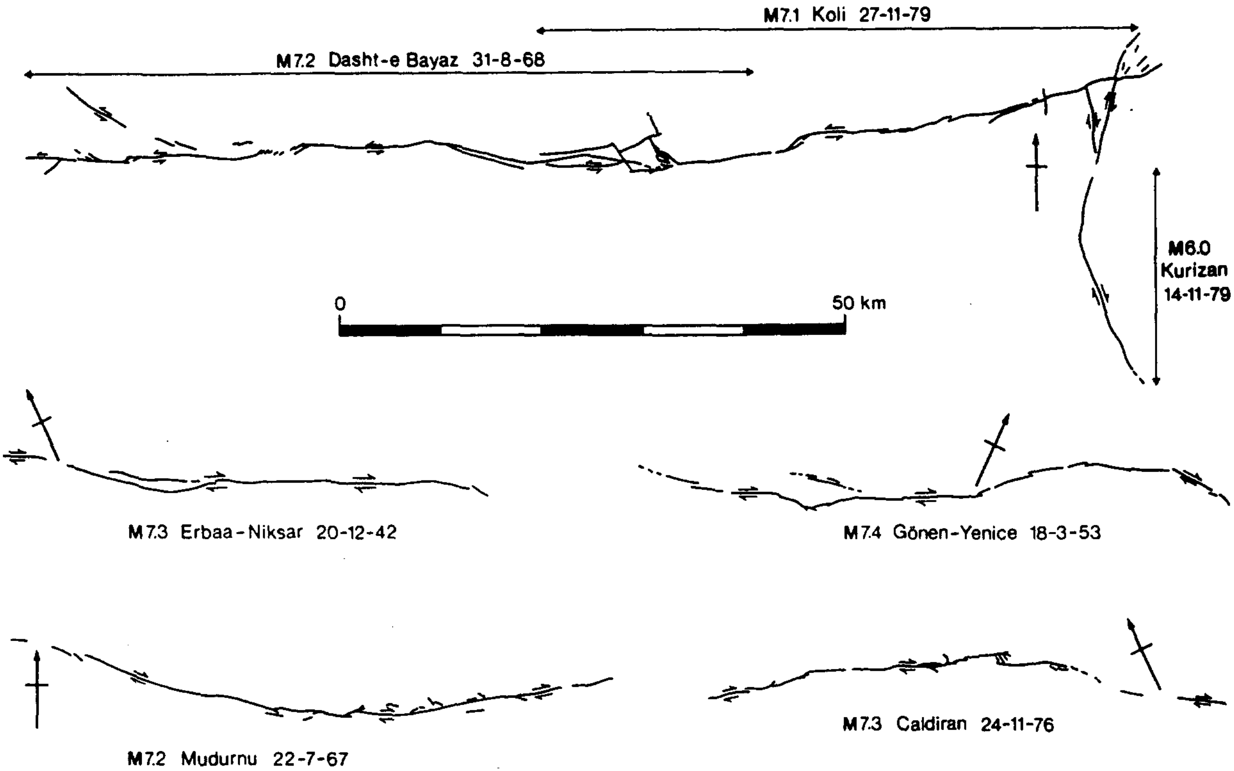

Fig. 5. Mapped surface traces of large predominantly strike-slip earthquake ruptures in Iran and Turkey. Above the scale bar are data for Iran, from Tchalenko & Barberian (1975) and Nowroozi & Mohajer-Ashjai (1985). Below the scale bar are data for Turkey from Ambraseys (1970) and Toksoz *et al.* (1977).

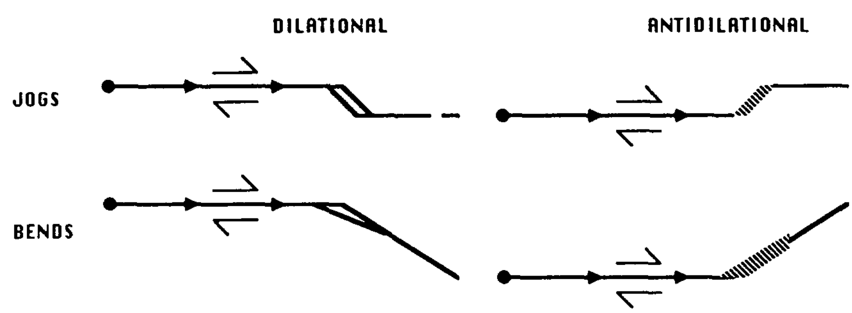

Fig. 6. Cartoon map of dilational and antidilational jogs and bends on a right-lateral strike-slip fault, with ruptures propagating from left to right. Solid circles represent earthquake epicentres.

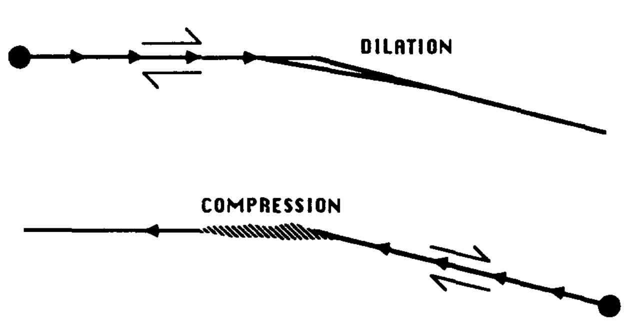

Fig. 7. Cartoon map illustrating the changing response of an isolated fault bend to rupture directivity on a right-lateral strike-slip fault. Solid circles represent earthquake epicentres.

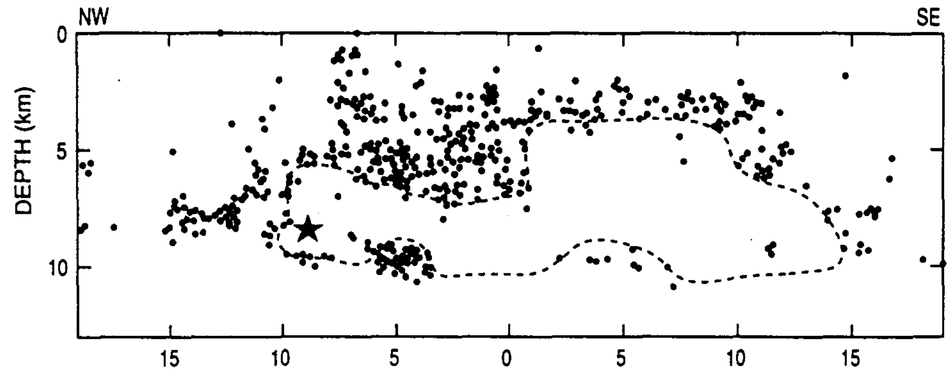

Fig. 8. Strike-parallel longitudinal profile of aftershocks with epicentres distributed within a 2.1 km wide tabular volume straddling the subvertical NW–SE strike-slip rupture associated with the 1984 M6.2 Morgan Hill earthquake (after Cockerham & Eaton 1987). Mainshock rupture (hypocentre — star) is believed to have occupied the area largely barren of aftershocks.

expand outwards with time (Fig. 8); and (ii) for ruptures breaking to the surface, aftershocks are few where the rupture trace is straight (that is, the rupture surface is planar), but tend to cluster adjacent to irregularities, especially near rupture terminations (Fig. 9).

The simple interpretation that emerges is that aftershocks largely represent the time-dependent response of the wallrocks to the sudden strains imposed by slip on an irregular mainshock rupture. Nur & Booker (1972) provided a plausible explanation for the occurrence and decay of aftershock activity involving the redistribution of aqueous fluids. Their hypothesis can be adapted to account for the observed location of many aftershock clusters in relation to fault irregularities. The seismogenic crust surrounding the mainshock rupture is likely to contain many subsidiary planes of weakness, with the stability of each plane determined by the standard Coulomb relationship,

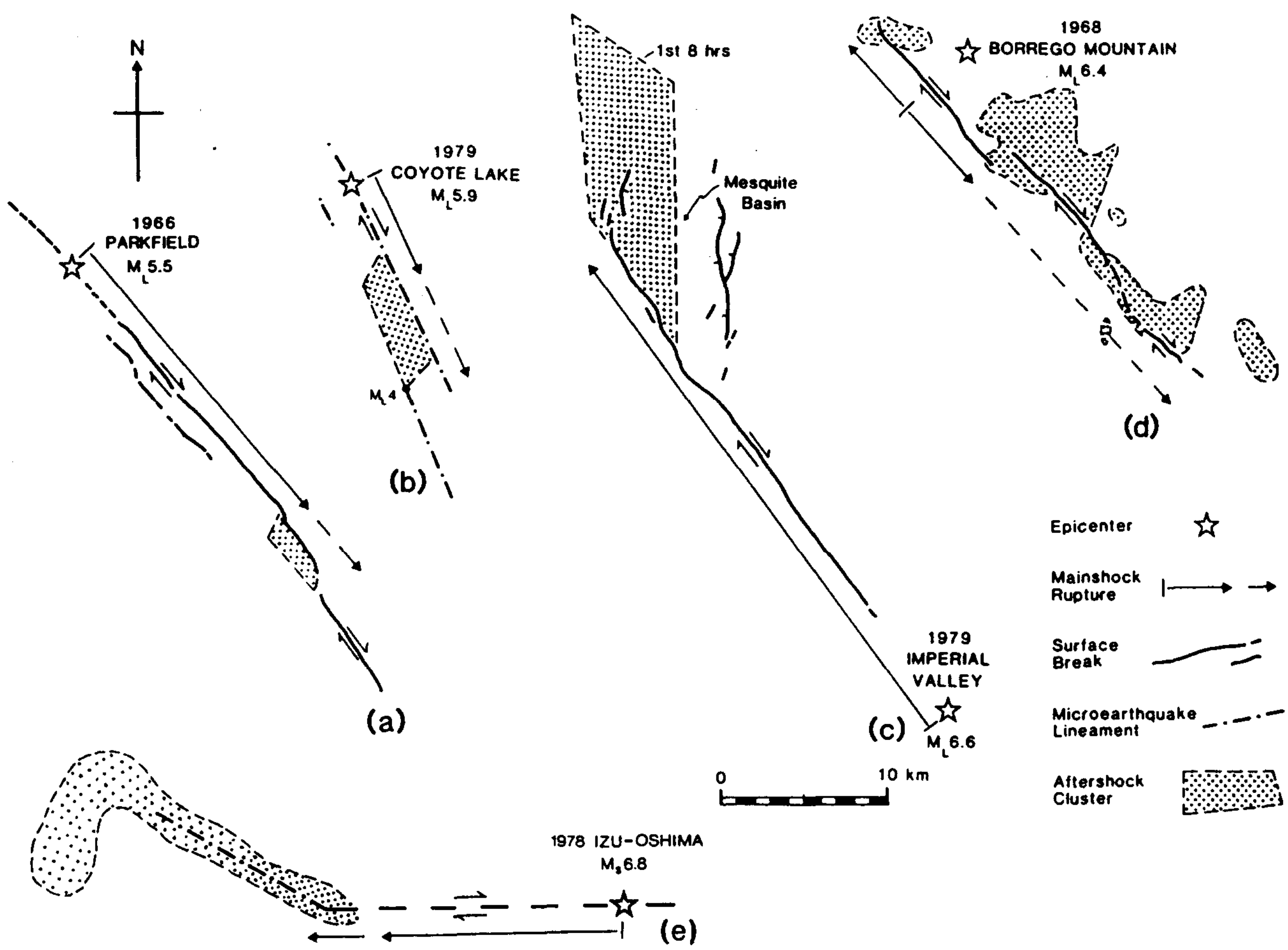

Fig. 9. Map view of aftershock epicentral clusters associated with irregular strike-slip ruptures. Events (a–d) occurred within the San Andreas fault system, California, respectively, on the San Andreas, Calaveras, Imperial and San Jacinto faults (see Sibson 1986b); event (e) near the Izu Peninsula, Japan, with the E–W mainshock rupture lying mostly offshore (Shimazaki & Somerville 1979).

$$\tau = C + \mu_s \sigma_n' = C + \mu_s(\sigma_n - P), \quad (5)$$

where τ and σ_n are respectively the shear and normal stress on the plane, P is the fluid pressure in the rock mass, C is the cohesion across the plane and μ_s is its coefficient of friction. Shear failure of these subsidiary planes could clearly be induced either by increasing τ, by decreasing σ_n or by increasing P. Earthquake faulting is accompanied by relief of shear stress along the central portions of the rupture and by concentration of shear stress at its ends (and to a lesser extent in remote locations equidistant from, and perpendicular to, the midpoint of the rupture plane; Das & Scholz 1981). Aftershocks are often concentrated at rupture terminations, but redistribution of shear stress alone does not explain the time-dependent nature of aftershock activity.

Nur & Booker (1972) suggested that changes in the level of mean stress (and thus, σ_n) induced by the mainshock rupture are of at least equal importance. Elasticity theory dictates that immediately after the main shock, local changes in mean stress (which may be comparable to the shear stress drop) would be matched by changes in fluid pressure. Thus, instantaneously there is no overall change in the shear resistance of subsidiary fractures. However, the fluid pressure imbalance thus created then leads to time-dependent shear failure in the regions of lowered mean stress in accordance with equation (5), as fluid pressure in those regions is progressively restored. The important implication is that aftershocks should cluster in regions where mean stress has been reduced by slip on the mainshock rupture. Support for the hypothesis comes from observed concentrations of aftershocks in dilational fault jogs and bends, and immediately outside antidilational jogs (Fig. 9). In all these areas the mean stress is likely to have been reduced by incremental slip transfer (Segall & Pollard 1980).

STRUCTURAL QUESTIONS POSED BY SEISMOLOGY

The dynamic rupture processes outlined above pose a number of interlinked structural questions which need to be answered if paleoseismic aspects of faulting are to be addressed by structural geologists. Only partial answers, at best, exist at present — the discussion below is thus necessarily limited. However, either singly or together the topics present fruitful avenues for future structural research.

Self-similarity

It has been recognized for some time that earthquake rupturing appears to be largely a scale invariant process; this is manifested by the near-constancy of stress drop over an enormous range of rupture dimensions. King (1983) suggested that this geometrically self-similar behavior, accounting for the general frequency-magnitude relationship, arises from the inherent tendency of natural fault systems to develop as *fractal* geometric sets (Mandelbrot 1977). There is, however, growing evidence that large earthquakes (those with rupture dimensions exceeding the depth of the seismogenic zone) and small earthquakes follow different scaling relationships and belong to different fractal sets (Scholz 1982, Shimazaki 1986). Indirectly, this provides further evidence for characteristic earthquake behaviour on individual fault segments.

With regard to these concepts of self-similar behavior, the familiar structural adage that '... small mimics large ...' takes on new significance, and invites investigation of the extent to which faults and fractures, and perhaps more complex structures such as thrust duplexes, develop in scale-invariant geometric sets. It is particularly important to establish the scale range over which self-similarity holds for different structures. Preliminary studies have already been made on the scale independence of roughness on natural fault surfaces (Scholz & Aviles 1986, Power *et al.* 1987), on particle size distributions within various fault gouges (Sammis *et al.* 1986), and on the size distribution of extension fractures (Segall & Pollard 1983a). Much more work of this kind is warranted.

Finite vs incremental aspect ratios for fault slip

The contrast between the aspect ratios for incremental and finite slip on faults illustrated by equations (1) and (2), respectively, may be revealing a fundamental property of the structures governing characteristic earthquake behavior. Consider a fault segment along which 'ideal' characteristic earthquakes occur. Multiple repetitions of the same characteristic rupture starting and stopping at the same points, each with the same incremental aspect ratio, will lead to a progressive increase in the cumulative ratio of slip to fault segment length (Fig. 10). However, this can only occur if distributed permanent strains of the same order as the finite aspect ratio (~10%) develop in the country rocks around the ends of the fault segment. Some idea of the longevity of particular structures giving rise to characteristic earthquake behavior may also be gained. If, for example, the characteristic strain release for each rupture was $\sim 10^{-4}$, then ~1000 such slip increments would be required to generate a finite aspect ratio, $u_f/L_f \sim 0.1$, if the rupture dimen-

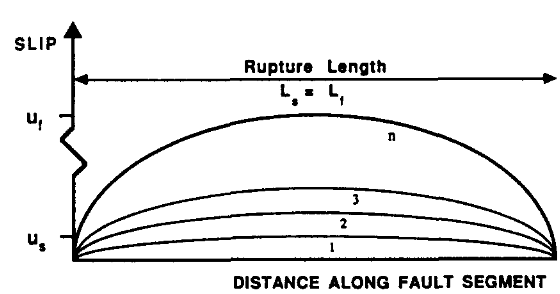

Fig. 10. Schematic diagram (not to scale) illustrating changing aspect ratios (cumulative slip/segment length) for a fault segment exhibiting ideal characteristic earthquake behaviour (partly after King 1986). u_s and u_f are, respectively, the incremental and cumulative values of maximum slip along the fault segment for a series of characteristic ruptures 1, 2, 3 ... n. L_s, rupture length; L_f, total fault length.

sions remain constant. Studies of changing aspect ratios as fault zones mature and evolve (e.g. Segall & Pollard 1983b, Walsh & Watterson 1988) are thus likely to yield important insights into the mechanics of faulting.

Starting and stopping controls

Fault segmentation leading to characteristic earthquake behavior demands the existence of persistent structural controls at segment boundaries, governing the nucleation and arrest of ruptures. An ability to recognize these structures would clearly be of immense value to seismic hazard assessment. Much effort has therefore been expended towards identifying rupture controls and understanding the mechanics of their operation. Attention has focused mostly on strike-slip fault systems where geometrical irregularities transverse to the direction of rupture propagation are defined in map view.

Although in some instance, there appears to be a correlation between well-located mainshock epicentres and fault bends or jogs (King & Nabelek 1985, King 1986), particularly of antidilational character, this is by no means always the case. Because larger ruptures generally initiate towards the base of the seismogenic zone, it seems probable that rheological as well as geometrical irregularities play an important role in the nucleation process (Sibson 1984). This further emphasizes the need for better understanding of the physical conditions and the very complex, mixed 'brittle–ductile' processes (e.g. Hobbs *et al.*, 1986, Sibson *et al.* 1988) prevailing in the vicinity of the FR/QP transition (see also discussion below).

A more consistent pattern of behavior is emerging with regard to rupture arrest. While antidilational jogs and bends clearly perturb ruptures and form obstacles to both incremental and long-term slip transfer along a fault, dilational fault jogs with cross-strike dimensions in excess of a kilometer or so seem to play an especially important role as preferred sites for rupture termination (Sibson 1986b, Knuepfer *et al.* 1987). This contrasts with expectations from the quasi-static elastic analysis of en échelon fault segmentation (Segall & Pollard 1980). Rupture arrest at dilational jogs is, however, generally followed by delayed slip transfer across the jog accompanied by localised aftershock activity (Fig. 9); these structures thus appear to act as kinetic barriers, impeding rapid but allowing slow slip transfer. Preliminary indications are that dilational bends likewise prove more effective as arresting structures than antidilational bends (Sibson 1987a). Given the directivity effect associated with isolated fault bends discussed earlier, this raises the intriguing possibility that such structures may act as one-way 'valves', forming a greater impediment to ruptures propagating in one direction than the other. One possible example of this behavior is the 'big-bend' on the San Andreas Fault (Fig. 2). The 1857 rupture is believed to have propagated from the NW to the SE with a significant drop in slip in the vicinity of the bend (Sieh 1978). However, whereas paleoseismic trenching at Wallace Creek (WC) northwest of the bend reveals three large slip (~10 m) events over the past 1000 years, trenches at Pallet Creek (PC) record six lesser slip events over roughly the same interval (Weldon & Sieh 1985). Thus, a plausible inference is that NW to SE propagating ruptures, though perturbed, continue around what to them is an antidilational bend, but SE to NW propagating 'catch-up' ruptures terminate at the bend because to them it acts as a dilational structure (Sibson 1987a).

Incremental slip transfer at the tips of propagating ruptures across both dilational jogs and bends involves forced extensional opening. Their time-dependent mechanical response to slip transfer is inferred to arise from the difficulty of forming substantial cavity space quickly in fluid-saturated crust. This is opposed by induced suctions, representing an extreme form of dilatancy hardening (Sibson 1986b). Evidence for this stopping mechanism and the special role of induced fluid pressure imbalances comes from the hydrothermal mineralization which is commonly localized in such dilational structural sites. The mineralization is often characterized by high-dilation, multiply recemented wallrock breccias that seem to have developed from the episodic hydraulic implosion of wallrock into fast-formed cavity space (Sibson 1987b).

These preliminary ideas on the structural control of ruptures should be treated with great caution. Many key questions remain to be answered. What is the relative importance of geometrical and rheological structural controls? Over what range of scales are geometrical irregularities effective? How do major fault irregularities come into being? What is their longevity in a particular configuration, and what factors affect this?

Directivity effects

When examining faults in the field, it is standard practice for structural geologists to attempt to determine the direction of slip, the sense of shear, and the amount of slip. However, little thought has so far been given to indicators that allow the direction of rupture propagation on faults during paleoslip events to be determined, though Hancock (1985) has speculated that asymmetric distributions of pinnate joints about faults may be related to directivity. Structural features diagnostic of rupture growth are widely recognized on joint surfaces, but these fractures are generally held (somewhat contentiously) to have formed by purely extensional opening (e.g. Engelder 1987). It might be expected that the tapering of slip along the fault slip direction for a single rupture event would tend to occur in the direction of rupture propagation. However, examination of the slip distribution deduced for the 1979 Imperial Valley earthquake (Fig. 4) and for other well-studied events show that this is generally not the case, since the area of maximum slip does not necessarily coincide with the site of rupture nucleation. Some other speculative ideas on structures that might be diagnostic of rupture directivity are as follows.

(1) Branching of ruptures is generally likely to occur

in the direction of rupture propagation (Bahat 1980, 1982). Such branching seems to have occurred, for example, during propagation of the normal-slip rupture accompanying the 1983 M7.3 Borah Peak earthquake in Idaho (Bruhn *et al.* 1987). Recognition of branching ruptures generated during a single paleoslip event may thus allow directivity to be assessed (cf. Fig. 4).

(2) For any isolated fault bend and sense of shear, substantial dilation of a fault segment is expected for only one of the two possible directions of rupture propagation (Fig. 7). The geometry of a hydrothermal cavity fill at an isolated bend thus has the potential to yield information on rupture directivity.

It is clear from the preceding discussion that rupture directivity may exert a significant control on the formation of cavity space at fault irregularities (see Fig. 7). The topic may thus have important implications for the development of fault-hosted mineralization.

Structures diagnostic of stress cycling

A great variety of minor structures, microstructural features and fault rock textures are found in association with fault zones (e.g. Sibson 1977, 1981, Hancock 1985, Hancock & Barka 1987). However, despite the recognized dominance of seismic slip episodes accommodating displacement in the upper crust, the general tendency has been to interpret fault-related structural features in terms of static stress fields. This arises in part because of textural overprinting in the vicinity of fault zones, but also because of the inherent difficulty of distinguishing fast from slow fracturing and cataclastic deformation. There has been only limited success to date in relating such features to dynamic rupture processes, or to other specific phases of the earthquake stress cycle.

Pseudotachylyte friction-melts on faults, and perhaps also the hydraulic implosion breccias found in dilational fault jogs, provide examples of fault rocks that are necessarily the products of the γ-phase of seismic slip (Sibson 1986a). However, interpreting the more common cataclastic rock products of the seismogenic regime (gouges, microbreccias and cataclasite series rocks) in terms of the earthquake stress cycle is often problematic. Undoubtedly many represent the rock products of frictional wear during seismic slip increments. Similar textures may, however, develop through aseismic cataclastic flow. As an example of the interpretative difficulties, one may consider the likely origin of the gouges and cataclasites with pronounced shape fabrics developed within tabular shear zones, such as those described by House & Gray (1982) and Chester & Logan (1986). It seems probable that the shape fabrics were imposed during slow aseismic shearing, but it remains unclear whether the shearing was stable aseismic, or might have been associated with δ-phase postseismic afterslip. There is also the possibility that vast patchy areas of distributed cataclastic deformation adjacent to major slip surfaces represent areas of intense aftershock activity and have little direct association to major shearing displacements (Sibson 1986b). The origin of the vast bulk of cataclastic rock products and their significance with respect to the seismic cycle thus remain enigmatic.

Repetitive microstructural sequences which probably result from the earthquake stress cycle are, however, becoming more widely recognised. The effects of the stress cycling around the base of the seismogenic regime are revealed by smeared-out pseudotachylytes, which provide evidence for transient loss of continuity accompanying the intermittent propagation of ruptures through mylonitic shear zones at mid-crustal depths (Sibson 1980, Passchier 1982, Hobbs *et al.* 1986). More subtle microstructural features in mylonites, interpreted as resulting from abrupt fluctuations in strain rate (White & White 1983, Knipe & Wintsch 1985), may have a similar origin. Crack–seal extension veining (Ramsay 1980, Cox & Etheridge 1982) is another widespread, cyclically developed microstructure that may plausibly be related to the earthquake stress cycle in at least some instances (Sibson 1981, Mawer & Williams 1985). Increments of extensional opening most probably accompanying successive β-phases of preseismic strain accumulation (see example below). This microstructure is also noteworthy for the important constraints it puts on local shear stress levels during faulting (Sibson 1981, Etheridge 1983).

Though at an early stage, diagnosis of fault rocks and minor fault structures in terms of the earthquake stress cycle is a challenging but worthwhile exercise for the added insight it may give into the physical conditions and mechanics of faulting.

SHEAR ZONE HOSTED MESOTHERMAL GOLD–QUARTZ LODES: AN EXAMPLE OF SEISMO-STRUCTURAL ANALYSIS

Mesothermal gold–quartz lodes hosted in steeply inclined shear zones of mixed 'brittle–ductile' character account for a significant proportion of global gold production. While these vein systems are best known from Archean granite–greenstone belts in Canada and elsewhere, younger deposits such as the Cretaceous Mother Lode system of California also occur in similar tectonic settings. They provide an instructive example of structures that, arguably, can only be understood in the context of their original situation with respect to the seismogenic regime and the stress cycling that occurs therein (Sibson *et al.* 1988). Structural relationships also put tight constraints on the shear stress levels driving the system.

The hosting shear zones have mostly developed under low- to mid-greenschist metamorphic conditions and exhibit mixed brittle–ductile characteristics with discrete shears and vein-fractures developing syntectonically with *L–S* shear zone fabrics. While many of the shear zones have clearly undergone a long and varied history of movement, shear sense indicators invariably show that the mineralization developed during a phase of late high-angle reverse or reverse-oblique slip. The veins contain mixed H_2O–CO_2 fluid inclusions of relatively

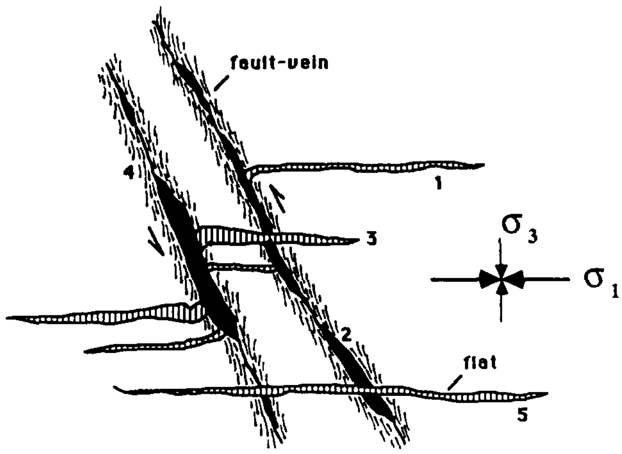

Fig. 11. Schematic evolutionary sequence (1–5) of prefailure *flats* (cross-hatched) alternating with postfailure discharge *fault-veins* (solid), illustrating the development of mutually cross-cutting vein-sets at Sigma Mine, Quebec (after Robert & Brown 1986). Note the problems in interpretation that would arise if only a few of the cross-cutting relationships between the vein sets were exposed.

low salinity, and carbonate alteration is often intense in their immediate vicinity. Studies of the fluid inclusions and the isotopic characteristics of the mineralization suggest that the deposits developed in the temperature range 250–400°C at pressures of 2–4 kbar (~7–14 km depth) (Kerrich 1986, Robert & Kelly 1987). The overall inference, therefore, is that the veining developed around the base of the seismogenic regime within the roots of brittle high-angle reverse or reverse-oblique fault systems. This is in marked contrast to epithermal gold–quartz mineralization which tends to develop at shallow depth in extensional or transtensional fault regimes.

Structural characteristics of these deposits are well exemplified by the Sigma Mine at Val d'Or in Quebec where a quartz–tourmaline vein system cutting andesitic meta-volcanics intruded by porphyritic diorite has been mapped in great detail (Robert & Brown 1986). A noteworthy feature of the veining here and in some of the other deposits is its great vertical extent (>2 km in several instances). Two main vein sets occur; lenticular *fault-veins* subparallel to the schistosity within almost pure reverse shear zones dipping steeply at about 70°, and *flats* (subhorizontal extension veins). Structural relationships between the vein sets are illustrated schematically in Fig. 11, together with the inferred stress field. Within each set, composite vein textures record histories of incremental deposition, the purely extensional character of the flats being revealed by repeated crack–seal increments. The key structural observation, however, is that there is no consistent cross-cutting relationship between the vein-sets (Robert & Brown 1986). This has the important implication that the two sets of veins developed at different stages of a repeating cycle.

Fault-valve model

From the high-angle reverse character of the shear zones and the observed structural relationships, we infer that they acted as fluid-pressure-activated *valves*, promoting repeated fluctuations in fluid pressure intimately linked to the earthquake stress cycle. Simple friction theory (Sibson 1985) shows that a necessary requirement for the reactivation of high-angle reverse faults at large reactivation angles (θ_r) is that fluid pressure exceeds the lithostatic load; the flats, formed by natural hydraulic fracturing, demonstrate that this was indeed the case from time to time. The following repeating cycle is envisaged (Sibson *et al.* 1988).

Fluid pressure around the base of the seismogenic zone builds up to supralithostatic values, with flats probably opening by hydraulic fracturing during the β preseismic phase of the stress cycle (Fig. 3). Shear failure then becomes possible and a reverse-slip rupture nucleates in the shear zone (γ-phase). The rupture propagates upwards through the seismogenic regime, relieving shear stress and creating fracture permeability along the fault. Post failure discharge from the geopressured reservoir at depth then occurs along the rupture zone with fluid pressures dropping rapidly towards hydrostatic values. Hydrothermal deposition occurs within 'ride-overs' to form lenticular fault veins during this post-seismic δ-phase of afterslip and aftershock activity. Discharge progressively diminishes, and hydrothermal self-sealing then allows the cycle to repeat.

In summary, therefore, the zones of extensional flats and discharge fault-veins appear to represent the nucleation sites of high-angle reverse ruptures, with the build-up and release of fluid pressure linked to different phases of the earthquake stress cycle. Inconsistent cross-cutting relationships between the fault-veins and the flats are a natural consequence of the cyclical process. Similar fault-valve behavior may perhaps be expected for other faults that are unfavorably oriented for reactivation.

Stress levels

Arguments can also be made that rupture events on the faults were initiated under low values of shear stress, τ_i. Continued reactivation of the high-angle reverse faults in preference to the formation of more favorably oriented thrusts (Sibson 1985), coupled with the presence of extensional flats formed by hydraulic fracturing (Etheridge 1983), constrains the shear stress to a value comparable to the tensile strength of the country rocks, probably no more than 100 bars at most. Thus the degree of stress relief accompanying rupturing is likely to have been high, with $\Delta\tau/\tau_i \rightarrow 1$.

DISCUSSION—FUTURE RESEARCH TRENDS

Earthquake faulting is an integral part of structural process within the upper continental crust. This paper has sought to demonstrate that proper understanding of fault structure requires an appreciation of the dynamic effects accompanying rupturing. Modern seismology raises many questions on fault processes, for example directivity effects, that are not usually considered by structural geologists investigating faults. Conversely, the geological structure of fault zones contains much information of potential interest to seismologists. Prime future goals in the structural investigation of fault zones must be the recognition of features that provide specific information on the stress levels accompanying faulting, on features diagnostic of the earthquake stress cycle, and on the dynamic processes accompanying faulting. Understanding the geometrical structure and mechanics of earthquake rupture controls is of particular importance. While much of what has been written has been concerned with strike-slip faulting, the concepts are equally applicable to dip-slip faults. It will be interesting, for example, to explore the role of flats and ramps in thrust systems as potential rupture controls.

The dynamic effects of seismic faulting are probably interwoven throughout much of geological process. Emphasis has been placed on their role in perturbing fluid flow and localizing fault-hosted mineralization, which appears to be of special importance. It seems likely that they may play an equally important role in the migration of hydrocarbon fluids. However, other fundamental processes such as erosion and sedimentation may also be affected. For example, particularly violent ground shaking is induced wherever a propagating rupture accelerates or decelerates. Episodic rupture arrest at a pull-apart basin occupying a dilational fault jog must therefore greatly influence the character of mass movement and sedimentation within the basin.

While a remarkable marriage of structural and seismological information has been achieved over just the past few years, there is clearly much scope for further integration of seismological information into our general understanding of structural and other fundamental geological processes. Much remains to be done.

Acknowledgements—I thank Ralph Archuleta, Tom Blenkinsop, Tom Hanks and Rob Knipe for reading various drafts of this manuscript, and Juan Watterson for especially perceptive criticism. Work leading to this paper was supported by National Science Foundation grant EAR86—07445 and U.S. Geological Survey grant 14-08-0001-G1331.

REFERENCES

Ambraseys, N. N. 1970. Some characteristic features of the Anatolian fault zone. *Tectonophysics* **9**, 143–165.

Andrews, D. J. 1980. A stochastic fault model. (I) Static case. *J. geophys. Res.* **85**, 3867–3877.

Archuleta, R. J. 1984. A faulting model for the 1979 Imperial Valley earthquake. *J. geophys. Res.* **89**, 4559–4585.

Bahat, D. 1980. Secondary faulting, a consequence of a single continuous bifurcation process. *Geol. Mag.* **117**, 373–380.

Bahat, D. 1982. Extensional aspects of earthquake induced ruptures by an analysis of fracture bifurcation. *Tectonophysics* **83**, 163–183.

Bakun, W. H. & McEvilly, T. V. 1984. Recurrence models and Parkfield, California, earthquakes. *J. geophys. Res.* **89**, 3051–3058.

Bruhn, R. L., Gibbler, P. R. & Parry, W. T. 1987. Rupture characteristics of normal faults; an example from the Wasatch fault zone, Utah. In: *Continental Extensional Tectonics* (edited by Coward, M. P., Dewey, J. F. & Hancock, P. L.). *Spec. Publs geol. Soc. Lond.* **28**, 337–353.

Burford, R. O. & Harsh, P. W. 1980. Slip on the San Andreas fault in central California from alinement array surveys. *Bull. seism. Soc. Am.* **30**, 1233–1261.

Chen, W. P. & Molnar, P. 1983. Focal depths of intracontinental and intraplate earthquakes and their implications for the thermal and mechanical properties of the lithosphere. *J. geophys. Res.* **88**, 4183–4214.

Chester, F. M. & Logan, J. M. 1986. Implications for mechanical properties of brittle faults from observations of the Punchbowl fault zone, California. *Pure & Appl. Geophys.* **124**, 77–106.

Cockerham, R. S. & Eaton, J. P. 1987. The earthquake and its aftershocks, April 24 through September 30, 1984. *Bull. U.S. geol. Surv.* **1639**, 15–28.

Cox, S. F. & Etheridge, M. A. 1982. Crack-seal fibre growth mechanisms and their significance in the development of oriented layer silicate microstructures. *Tectonophysics* **92**, 147–170.

Das, S. & Scholz, C. H. 1981. Off-fault aftershock clusters caused by shear stress increase? *Bull. seism. Soc. Am.* **71**, 1669–1675.

Engelder, T. 1987. Joints and shear fractures in rocks. In: *Fracture Mechanics of Rock* (edited by Atkinson, B. K.). Academic Press, London, 27–69.

Etheridge, M. A. 1983. Differential stress magnitudes during regional deformation and metamorphism — upper bound imposed by tensile fracturing. *Geology* **11**, 231–234.

Gibowicz, S. J. 1973. Stress drop and aftershocks. *Bull. seism. Soc. Am.* **63**, 1433–1446.

Gutenberg, B. & Richter, C. F. 1944. Frequency of earthquakes in California. *Bull. seism. Soc. Am.* **34**, 186–188.

Hancock, P. L. 1985. Brittle microtectonics — principles and practice. *J. Struct. Geol.* 7, 437–457.

Hancock, P. L. & Barka, A. A. 1987. Kinematic indicators on active normal faults in western Turkey. *J. Struct. Geol.* **9**, 573–584.

Hanks, T. C. 1977. Earthquake stress drops, ambient tectonic stresses, and stresses that drive plate motions. *Pure & Appl. Geophys.* **115**, 441–458.

Hanks, T. C. & Kanamori, H. 1979. A moment-magnitude scale. *J. geophys. Res.* **84**, 2348–2350.

Hanks, T. C. & Raleigh, C. B. 1980. The conference on magnitude of deviatoric stresses in the Earth's crust and upper mantle. *J. geophys. Res.* **85**, 6083–6085.

Hobbs, B. E., Ord, A. & Teyssier, C. 1986. Earthquakes in the ductile regime? *Pure & Appl. Geophys.* **124**, 309–336.

House, W. M. & Gray, D. R. 1982. Cataclasites along the Saltville thrust, U.S.A., and their implications for thrust sheet emplacement. *J. Struct. Geol.* **4**, 257–269.

Hyndman, R. D. & Weichert, D. H. 1983. Seismicity and rates of relative motion along the plate boundaries of western North America. *Geophys. J. R. astr. Soc.* **72**, 59–82.

Jennings, C. W. 1975. Fault map of California, 1:750,000. *Calif. Div. Mines Geol.* Geologic Data Map No. 1.

Johnson, C. E. & Hutton, L. K. 1982. Aftershocks and pre-earthquake seismicity, the Imperial Valley, California, earthquake, October 15, 1979. *Prof. Pap. U.S. geol. Surv.* **1254**, 59–76.

Kanamori, H. & Anderson, D. L. 1975. Theoretical basis of some empirical relationships in seismology. *Bull. seism. Soc. Am.* **65**, 1073–1095.

King, G. C. P. 1978. Geological faults, fracture, creep and strain. *Phil. Trans. R. Soc. Lond.* **A288**, 197–212.

King, G. C. P. 1983. The accommodation of large strains in the upper lithosphere of the earth and other solids by self-similar fault systems — the geometrical origin of *b*-value. *Pure & Appl. Geophys.* **121**, 762–815.

King, G. C. P. 1986. Speculations on the geometry of the initiation and termination processes of earthquake rupture and its relation to morphology and geological structure. *Pure & Appl. Geophys.* **124**, 567–585.

King, G. C. P. & Nábelek, J. 1985. The role of bends in faults in the initiation and termination of earthquake rupture. *Science* **228**, 984–987.

King, G. C. P. & Vita-Finzi, C. 1981. Active folding in the Algerian earthquake of 10 October 1980. *Nature* **292**, 22–26.

Kerrich, R. 1986. Fluid infiltration into fault zones: chemical, isotopic, and mechanical effects. *Pure & Appl. Geophys.* **124**, 226–268.

Knipe, R. J. & Wintsch, R. P. 1985. Heterogeneous deformation, foliation development, and metamorphic processes in a polyphase mylonite. In: *Metamorphic Reactions — Kinetics, Textures and Deformation* (edited by Thompson, A. B. & Rubie, D. C.). Springer-Verlag, New York, 180–210.

Knuepfer, P. L. K., Bamberger, M. J., Turko, J. M. & Coppersmith, K. J. 1987. Characteristics of the boundaries of historical surface fault ruptures. *Seism. Res. Lett.* **58**, 31.

Mandelbrot, B. 1977. *Fractals: Form, Chance and Dimension.* W. H. Freeman, San Francisco.

Mavko, G. M. 1981. Mechanics of motion on major faults. *Ann. Rev. Earth Planet. Sci.* **9**, 81–111.
Mawer, C. K. & Williams, P. F. 1985. Crystalline rocks as possible paleoseismicity indicators. *Geology* **13**, 100–102.
Molnar, P. 1979. Earthquake recurrence intervals and plate tectonics. *Bull. seism. Soc. Am.* **69**, 115–133.
Moore, J. G. & du Bray, E. 1978. Mapped offset on the right-lateral Kern Canyon fault, southern Sierra Nevada, California. *Geology* **6**, 205–208.
Nowroozi, A. A. & Mohajer-Ashjai, A. 1985. Fault movement and tectonics of eastern Iran: boundaries of the Lut plate. *Geophys. J. R. astr. Soc.* **83**, 215–237.
Nur, A. & Booker, J. R. 1972. Aftershocks caused by pore fluid flow? *Science* **175**, 885–887.
Oppenheimer, D. H., Reasenberg, P. A. & Simpson, R. W. 1988. Fault plane solutions for the 1984 Morgan Hill, California, earthquake sequence: evidence for state of stress on the Calaveras fault. *J. geophys. Res.* **93**, 9007–9026.
Passchier, C. W. 1982. Pseudotachylyte and the development of ultramylonite bands in the Saint-Barthelemy Massif, French Pyrenees. *J. Struct. Geol.* **4**, 69–79.
Power, W. L., Tullis, T. E. & Weeks, J. D. In press. Roughness and wear during brittle faulting. *J. geophys. Res.*
Ramsay, J. G. 1980. The crack–seal mechanism of rock deformation. *Nature* **284**, 135–139.
Reasenberg, P. & Ellsworth, W. L. 1982. Aftershocks of the Coyote Lake, California, earthquake of August 6, 1979: a detailed study. *J. geophys. Res.* **87**, 10,637–10,655.
Reid, H. F. 1911. The elastic-rebound theory of earthquakes. *Univ. Calif. Publ. Geol. Sci.* **6**, 413–444.
Rikitake, T. 1975. Statistics of ultimate strain of the earth's crust and probability of earthquake occurrence. *Tectonophysics* **26**, 1–21.
Robert, F. & Brown, A. C. 1986. Archean gold-bearing quartz veins at the Sigma Mine, Abitibi greenstone belt, Quebec: Part 1 — Geologic relations and formation of the vein system. *Econ. Geol.* **81**, 578–592.
Robert, F. & Kelly, W. C. 1987. Ore-forming fluids in Archean gold-bearing quartz veins at the Sigma Mine, Abitibi greenstone belt, Quebec, Canada. *Econ. Geol.* **82**, 56–74.
Sammis, C. G., Osborne, R. H., Anderson, J. L., Banerdt, M. & White, P. 1986. Self-similar cataclasis in the formation of fault gouge. *Pure & Appl. Geophys.* **124**, 53–78.
Scholz, C. H. 1977. Transform fault systems of California and New Zealand: similarities in their tectonic and seismic styles. *J. geol. Soc. Lond.* **133**, 215–230.
Scholz, C. H. 1982. Scaling laws for large earthquakes: consequences for physical models. *Bull. seism. Soc. Am.* **72**, 1–14.
Scholz, C. H. 1988. The brittle–plastic transition and the depth of seismic faulting. *Geol. Rdsch.* **77**, 319–328.
Scholz, C. H. & Aviles, C. H. 1986. The fractal geometry of faults and faulting. In: *Earthquake Source Mechanics* (edited by Das, S., Boatwright, J. & Scholz, C. H.). *Am. Geophys. Un. Geophys. Monogr.* **37** *(Maurice Ewing Series* **6**), 147–155.
Schwartz, D. P. & Coppersmith, K. J. 1984. Fault behavior and characteristic earthquakes: examples from the Wasatch and San Andreas fault zones. *J. geophys. Res.* **89**, 5681–5698.
Segall, P. & Pollard, D. D. 1980. Mechanics of discontinuous faults. *J. geophys. Res.* **85**, 4337–4350.
Segall, P. & Pollard, D. D. 1983a. Joint formation in granitic rocks of the Sierra Nevada. *Bull. geol. Soc. Am.* **94**, 563–575.
Segall, P. & Pollard, D. D. 1983b. Nucleation and growth of strike-slip faults in granite. *J. geophys. Res.* **88**, 555–568.
Shimazaki, K. 1986. Small and large earthquakes: the effects of the thickness of seismogenic layer and the free surface. In: *Earthquake Source Mechanics* (edited by Das, S., Boatwright, J. & Scholz, C. H.). *Am. Geophys. Un. Geophys. Monogr.* **37** (Maurice Ewing Series **6**), 147–155.
Shimazaki, K. & Somerville, P. 1979. Static and dynamic parameters of the Izu-Oshima, Japan, earthquake of January 14, 1978. *Bull. seism. Soc. Am.* **69**, 1343–1378.
Sibson, R. H. 1977. Fault rocks and fault mechanisms. *J. geol. Soc. Lond.* **133**, 191–214.
Sibson, R. H. 1980. Transient discontinuities in ductile shear zones. *J. Struct. Geol.* **2**, 165–171.
Sibson, R. H. 1981. Fluid flow accompanying faulting: field evidence and models. In: *Earthquake Prediction: an International Review* (edited by Simpson, D. W. & Richards, P. G.). *Am. Geophys. Un. Maurice Ewing Series* **4**, 593–603.
Sibson, R. H. 1983. Continental fault structure and the shallow earthquake source. *J. geol. Soc. Lond.* **140**, 741–767.
Sibson, R. H. 1984. Roughness at the base of the seismogenic zone: contributing factors. *J. geophys. Res.* **89**, 5791–5799.
Sibson, R. H. 1985. A note on fault reactivation. *J. Struct. Geol.* **7**, 751–754.
Sibson, R. H. 1986a. Earthquakes and rock deformation in crustal fault zones. *Ann. Rev. Earth Planet. Sci.* **14**, 149–175.
Sibson, R. H. 1986b. Earthquakes and lineament infrastructure. *Phil. Trans. R. Soc. Lond.* **A317**, 63–79.
Sibson, R. H. 1987a. Effects of fault heterogeneity on rupture propagation. *U.S. Geol. Surv. Open-File Report* **87–673**, 362–373.
Sibson, R. H. 1987b. Earthquake rupturing as a hydrothermal mineralizing agent. *Geology* **15**, 701–704.
Sibson, R. H., Robert, F. & Poulsen, K. H. 1988. High-angle reverse faults, fluid pressure cycling and mesothermal gold-quartz deposits. *Geology* **16**, 551–555.
Sieh, K. E. 1978. Slip along the San Andreas fault associated with the great 1857 earthquake. *Bull. seism. Soc. Am.* **68**, 1421–1448.
Silver, P & Masuda, T. 1985. A source extent analysis of the Imperial Valley earthquake of October 15, 1979, and the Victoria earthquake of June 9, 1980. *J. geophys. Res.* **90**, 7639–7651.
Stein, R. S. & King, G. C. P. 1984. Seismic potential revealed by surface folding — the 1983 Coalinga, California, earthquake. *Science* **224**, 869–872.
Strehlau, 1986. A discussion of the depth extent of rupture in large continental earthquakes. In: *Earthquake Source Mechanics* (edited by Das, S., Boatwright, J. & Scholz, C. H.). *Am. Geophys. Un. Geophys. Monogr.* **37** *(Maurice Ewing Series* **6**), 147–155.
Tchalenko, J. S. & Berberian, M. 1975. Dasht-e-Bayaz fault, Iran: earthquake and earlier related structures in bedrock. *Bull. geol. Soc. Am.* **86**, 703–709.
Toksoz, M. N., Arpat, E. & Saroglu, F. 1977. East Anatolian earthquake of 24 November, 1976. *Nature* **270**, 423–425.
Vedder, J. G. & Wallace, R. E. 1973. Map showing recently active fault breaks along the San Andreas and related faults between Cholame Valley and Tejon Pass, California, Scale 1:24,000. *Geol. Misc. Invest. Map* **1–574**, U.S. Geol. Surv., Reston, Virginia.
Walsh, J. J. & Watterson, J. 1988. Analysis of the relationship between displacements and dimensions of faults. *J. Struct. Geol.* **10**, 239–247.
Watterson, J. 1986. Fault dimensions, displacements and growth. *Pure & Appl. Geophys.* **124**, 365–373.
Weldon, R. J. & Sieh, K. E. 1985. Holocene rate of slip and tentative recurrence interval for large earthquakes on the San Andreas fault, Cajon Pass, southern California. *Bull. geol. Soc. Am.* **96**, 793–812.
Wesnousky, S. G., Scholz, C. H., Shimazaki, K. & Matsuda, T. 1983. Earthquake frequency distribution and the mechanics of faulting. *J. geophys. Res.* **88**, 9331–9340.
White, J. C. & White, S. H. 1983. Semi-brittle deformation within the Alpine fault zone, New Zealand. *J. Struct. Geol.* **5**, 579–589.